Perspective: The first ten years of broadband chirped pulse Fourier transform microwave spectroscopy

G. Barratt Park and Robert W. Field

Citation: The Journal of Chemical Physics **144**, 200901 (2016); doi: 10.1063/1.4952762
View online: http://dx.doi.org/10.1063/1.4952762
View Table of Contents: http://scitation.aip.org/content/aip/journal/jcp/144/20?ver=pdfcov
Published by the AIP Publishing

Perspective: The first ten years of broadband chirped pulse Fourier transform microwave spectroscopy

G. Barratt Park[1,2,a)] and Robert W. Field[3,b)]
[1]*Institute for Physical Chemistry, University of Göttingen, Tammannstraße 6, 37077 Göttingen, Germany*
[2]*Max Planck Institute for Biophysical Chemistry, Göttingen, Am Faßberg 11, 37077 Göttingen, Germany*
[3]*Department of Chemistry, Massachusetts Institute of Technology, Cambridge, Massachusetts 02139, USA*

(Received 3 April 2016; accepted 16 May 2016; published online 27 May 2016)

Since its invention in 2006, the broadband chirped pulse Fourier transform spectrometer has transformed the field of microwave spectroscopy. The technique enables the collection of a ≥10 GHz bandwidth spectrum in a single shot of the spectrometer, which allows broadband, high-resolution microwave spectra to be acquired several orders of magnitude faster than what was previously possible. We discuss the advantages and challenges associated with the technique and look back on the first ten years of chirped pulse Fourier transform spectroscopy. In addition to enabling faster-than-ever structure determination of increasingly complex species, the technique has given rise to an assortment of entirely new classes of experiments, ranging from chiral sensing by three-wave mixing to microwave detection of multichannel reaction kinetics. However, this is only the beginning. Future generations of microwave experiments will make increasingly creative use of frequency-agile pulse sequences for the coherent manipulation and interrogation of molecular dynamics. *Published by AIP Publishing.* [http://dx.doi.org/10.1063/1.4952762]

I. INTRODUCTION

It is not every day that a scientific innovation leads to a >1000-fold improvement in the rate at which data can be acquired. An innovation of this magnitude is transformative. What could previously be measured in 3 yr can now be measured in a single day. What is even more unusual is that such an innovation could take place in a field that is almost a century old. The invention of chirped pulse Fourier transform microwave (CP-FTMW) spectroscopy by the Pate group at the University of Virginia is exactly this kind of innovation.[1,2] By increasing the shot-by-shot bandwidth of Fourier transform microwave spectroscopy from ~0.5 MHz to >10 GHz, the CP-FTMW technique has increased the rate at which broadband spectral information can be acquired in the microwave region by orders of magnitude.

Microwave spectroscopy is a technique that should delight every chemist. The resolving power is incredible. Gas-phase microwave experiments routinely achieve frequency resolution better than 10 kHz, so that a typical full-band spectrum covering 8–18 GHz contains (10 GHz/10 kHz) = 10^6 resolution elements. A chemical species can therefore be easily and unambiguously resolved and identified, even in complex mixtures. Furthermore, to zeroth order, the pattern of frequencies is directly related to the molecular geometry, and the spectrum can be directly compared with theoretical structure calculations. In almost no other form of spectroscopy is the relationship between geometric structure and spectrum so clear and so precise. Finally, hyperfine splittings and Stark effect microwave measurements provide direct high-precision probes into the most fundamental properties of the electronic wavefunction. Yet, despite its chemical appeal, microwave spectroscopy is not generally taught in the undergraduate chemistry classroom.

In some ways, the key advantages of microwave spectroscopy—extremely high resolution and precision—have also been a hindrance to its widespread use in the chemistry community. Because the broadband spectrum typically contains more than a million resolution elements, the spectrum must be scanned at high resolution, which requires hours or even days of continuous operation with traditional instruments. For this reason, microwave spectroscopy is not traditionally viewed as a survey technique for obtaining a "chemist's view" of a system. On the contrary, high-resolution narrow-band microwave scans require one to look at a very precise, restricted subset of information. With such a technique, one must know what one is looking for in order to find it, and when one only finds what one is looking for, one is rarely surprised.

However, with the invention of CP-FTMW spectroscopy, it is possible to collect 10^6 resolution elements in every shot of the spectrometer. Gas phase structure determinations of ever larger species, including dipeptides[3] and water decamers,[4] are being made at faster-than-ever rates. Microwave spectroscopy is being used to probe chemical kinetics and reaction dynamics.[5,6] Double-resonance experiments are being multiplexed for fast, unambiguous spectral diagnostics.[7,8] Finally, new coherent techniques based on frequency-agile pulse sequences are being explored,[9,10] which are reminiscent of the array of coherent experiments that are commonplace in Fourier transform nuclear magnetic resonance (FT-NMR). Certainly, the transformative results of the CP-FTMW innovation are already being felt, but the best is undoubtedly still to come.

a)Electronic mail: barratt.park@mpibpc.mpg.de
b)Electronic mail: rwfield@mit.edu

When one follows the progress that is being made, it seems that researchers are just beginning to make the paradigm shifts that are necessary to take full advantage of the new opportunities.

II. BACKGROUND AND HISTORY

Following the development of pulsed NMR techniques in the early 1950s (which eventually gave rise to FT-NMR), the microwave spectroscopy community began to exploit transient free induction decay (FID) phenomena, both as a means of achieving higher measurement sensitivity and to perform time-domain experiments on new areas of chemical physics such as rotational relaxation mechanisms. A variety of methods were employed, based on microwave pulsing,[11–14] frequency switching,[15] Stark switching,[16–19] and fast passage.[20–22] Like FT-NMR, microwave FID emission is a fully coherent phenomenon. Thus, the FID is emitted in the propagation direction of the incident electromagnetic wave, and the signal from a transition between two individual (J, M_J) sublevels is maximized when it is optimally polarized by an effective pulse angle of $\pi/2$.

In 1979, Balle and Flygare combined a pulsed microwave source with a tunable high quality Fabry-Pérot cavity, into which a molecular sample was introduced via a supersonic expansion.[23,24] A Fabry-Pérot cavity is an open resonator cavity surrounded by two (typically confocal) mirrors. When the distance between the mirrors, d, is a half-integer multiple of the wavelength ($d = n\lambda/2$), electromagnetic radiation of wavelength λ is constructively reinforced, creating resonant standing waves. The quality (Q) of the cavity can be defined in the frequency domain as $Q = \nu/\Delta\nu_c$, where ν is the center frequency of the resonator and $\Delta\nu_c$ is the bandwidth of radiation that is passively amplified by the cavity. Simple Fourier transform considerations indicate that $\tau_c = (2\pi\Delta\nu_c)^{-1}$ is the amount of time the average photon spends in the cavity. If we consider the cavity as a multi-pass system with N_p passes, then

$$Q = 2\pi N_p d/\lambda. \tag{1}$$

In other words, $Q\lambda/2\pi$ is the effective multipass length of the cavity.

The performance characteristics of the resulting Balle-Flygare Fourier-transform microwave (FTMW) spectrometer provided a remarkable leap forward. The high quality cavity and background-free detection scheme resulted in unprecedented sensitivity, while the collision-free, Doppler-narrow characteristics of the jet expansion and absence of power broadening gave rise to extremely narrow linewidths. The jet expansion also provided rotationally and configurationally cold conditions, which allowed the study of weakly bound complexes and which were crucial for extending microwave spectroscopy to larger systems with intractably large room-temperature partition functions. Finally, the cavity could be mechanically tuned over a wide (multi-octave) range, providing broadband search capability. Although the high quality (typically $Q = 10^4$) limits the instantaneous cavity bandwidth to $\Delta\nu_c = \nu/Q \approx 1$ MHz (for a typical $\nu = 10$ GHz carrier frequency), the tuning of the cavity to each carrier frequency can be automated so that the spectrometer can be scanned via software over its full operating range. The Balle-Flygare spectrometer ushered in a heyday for the field of microwave spectroscopy. What once had been primarily a tool for investigating individual transitions in small, stable molecules could now be used routinely to study weakly bound complexes,[25–28] to search for trace reactive intermediates or astronomically relevant species,[29,30] or to acquire rich broadband spectra of larger molecules,[31,32] with sufficient frequency resolution to observe hyperfine splittings due to nuclear quadrupole or nuclear spin-spin interactions.

The invention of broadband CP-FTMW by the Brooks Pate research group in 2006 transformed the field once more, again opening the door for entirely new classes of experiments. The Pate group took advantage of new technology to design a Fourier transform spectrometer that uses a high-power (>1 kW) chirped (frequency-swept) microwave pulse to polarize simultaneously all transitions that lie within a broad (>10 GHz) spectral region, and to detect and average the resulting broadband FID in the time domain on a fast oscilloscope. Chirping the frequency allows the broadband pulse to be "stretched" in time so that it delivers sufficient power at each frequency. Using this technique—which is, quite obviously, incompatible with the narrowband cavity used in the Balle-Flygare approach—a microwave spectrum spanning an entire octave of frequency

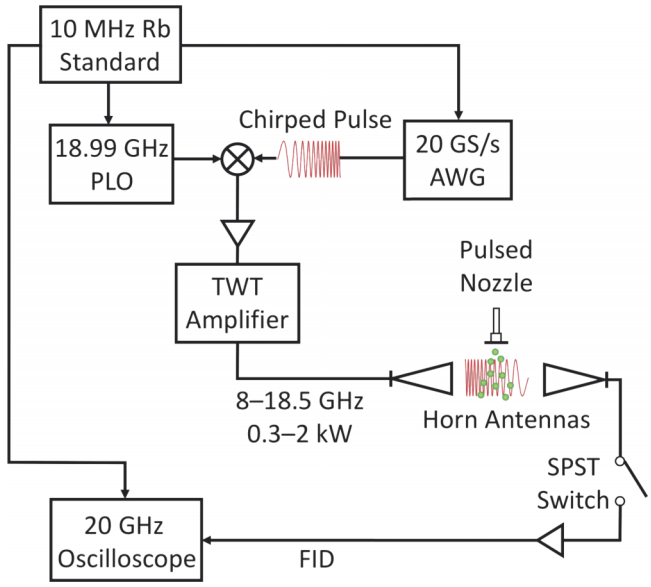

FIG. 1. Schematic diagram of the chirped pulse instrument design, following Fig. 1.B of Ref. 1. A broadband chirped pulse (0.5–10 GHz) is generated by a fast arbitrary waveform generator (AWG) and up-converted to 8–18.5 GHz by mixing with a phase locked oscillator (PLO). The resulting pulse is amplified by a traveling wave tube (TWT) amplifier to a power of 0.3–2 kW and coupled into a vacuum chamber via a set of matching horn antennas, where it polarizes all transitions in the molecular sample that fall within the chirp bandwidth. After the excitation pulse, the molecules emit an FID, which is amplified and detected on a fast oscilloscope. A single-pole single-throw (SPST) switch protects the detection arm from the high power excitation pulse. To enable averaging in the time domain, all frequency generating components are phase-locked to the same 10 MHz Rb standard.

can be acquired in a single shot, and multiple shots can be averaged in the time domain. In contrast, the Balle-Flygare spectrometer acquires only ~0.5 MHz of spectrum at a time, and the cavity must be mechanically tuned and optimized ~20 000 times in order to scan through the full range of the spectrometer, a process which is time-consuming, and which introduces uncertainty in relative intensities. Figure 1 is a schematic diagram of the Pate spectrometer design.

III. THEORY

As in cavity-FTMW spectroscopy, the macroscopic polarization obtained in CP-FTMW spectroscopy is described in the two-level system density matrix formalism by the optical Bloch equations, analogous to the Bloch equations used to describe the magnetic polarization in NMR. The optical Bloch equations include phenomenological relaxation rates T_1^{-1} (for decay of the population difference to its equilibrium value) and T_2^{-1} (for decay of coherence), which limit the duration of the FID emission. For experiments performed in a waveguide cell, it is typically assumed that all collisions are hard (population changing) collisions, and typically $T_1^{-1} = T_2^{-1} \approx 10$ MHz/Torr. Under molecular jet expansion conditions, however, the FID lifetime is determined by the Doppler limited T_2 coherence time, whereas $T_1 \gg T_2$ and is unimportant. Because the FID cannot be detected until after the end of the excitation pulse, the duration of the pulse, t_p, must be short relative to T_2, to avoid the loss of signal that decays during the excitation pulse. Typically, pulse durations of $t_p \approx 1$ μs are employed. The pulse power should be high enough to achieve a sufficient degree of polarization of each transition within the chirp bandwidth. This requires the use of high-power amplifiers (typically 1–1000 W for a 10 GHz bandwidth, depending on the molecular dipole moment and on the spectrometer design).

The polarization response that results from a chirped excitation pulse of the form

$$E = 2\mathcal{E}\cos\left(\omega_i t + \frac{1}{2}\alpha t^2\right), \tag{2}$$

where ω_i is the initial frequency, α is the rate of frequency sweep, and $\mathcal{E}$ is the magnitude of the oscillating electric field, is more complicated than that obtained from a narrow-band pulse with a constant carrier frequency. However, the physics is exactly analogous to that of the polarization response obtained in Stark sweeping experiments performed in the 1970s,[20–22] where the resonance frequency is swept through the frequency of a fixed microwave source, by switching on a voltage across a pair of Stark plates. McGurk and Flygare derived an analytical result for the weak excitation field limit, where the Rabi frequency is slow relative to the sweep rate (i.e., $\mu_{ab}\mathcal{E}/\hbar\alpha^{1/2} \ll 1$) so that population transfer is negligible.[22,33] In this limit, if we assume that $t_p \ll T_2$ and that the resonance frequency (ω_0) is sufficiently far away from the initial and final frequencies of the chirped pulse to avoid "edge effects" ($|\omega_i - \omega_0|, |\omega_f - \omega_0| \gg \sqrt{\pi\alpha}$),[34] then the magnitude of the polarization response, $|P|$, for each transition within the chirped excitation pulse is given by

$$|P| = \frac{2|\mu_{ab}|^2\mathcal{E}\Delta N_0}{\hbar}\sqrt{\frac{\pi}{\alpha}} \qquad \text{(weak field limit)}, \tag{3}$$

where ΔN_0 is the initial population difference of the two-level system.

It is instructive to consider the polarization response qualitatively in the rotating Bloch sphere picture. To be rigorous, one must sum the polarization response over the contribution of each of the degenerate M_J sub-levels to the polarization to account for the M_J-dependence of $|\mu_{ab}|$, but we confine our description to a simple two-level system. Following the definitions given by Allen and Eberly,[35] the Bloch vector $\boldsymbol{\Theta}$, with components u, v, w, is a representation of the density matrix of the system, in a frame of reference that rotates at the frequency ω of the incident excitation field. The vertical w component represents the instantaneous population difference $\rho_{aa} - \rho_{bb}$, and the magnitude of the projection of $\boldsymbol{\theta}$ onto the v, w plane is proportional to the magnitude of the coherent polarization. u and v are the in-phase and quadrature components, respectively, of the polarization with respect to the driving field. In the rotating wave approximation, the dynamics of the system obey the equation

$$\frac{d\boldsymbol{\Theta}}{dt} = \boldsymbol{\Omega} \times \boldsymbol{\Theta}, \tag{4}$$

where the driving vector, $\boldsymbol{\Omega}$, has the components

$$\boldsymbol{\Omega} = (-\mu_{ab}\mathcal{E}/\hbar, 0, \omega_0 - \omega). \tag{5}$$

According to Eq. (4), the driving vector $\boldsymbol{\Omega}$ describes the torque on the Bloch vector $\boldsymbol{\theta}$. The Bloch vector $\boldsymbol{\theta}$ will precess about the driving vector at a rate given by $|\Omega| = [(\mu_{ab}\mathcal{E}/\hbar)^2 + (\omega_0 - \omega)^2]^{1/2}$, which is the off-resonance Rabi frequency.

Figure 2 is based on Fig. 4 of Ref. 36, which provides a nice description of the chirped pulse polarization response in the Bloch sphere picture. The top row of Fig. 2 shows the behavior of the system in the narrow-band excitation limit (employed in cavity-FTMW experiments). The $\boldsymbol{\theta}$ vector points initially along the vertical axis, representing an initial population difference (no coherence at $t = 0$). The driving field is narrow and can be represented by a single frequency, very close to resonance, so $\boldsymbol{\Omega}$ lies along the u axis. The $\boldsymbol{\theta}$ vector thus experiences a torque about the u axis at the on-resonance Rabi frequency, and exhibits characteristic Rabi-cycling behavior.

The middle row of Fig. 2 shows the chirped pulse response in the weak driving field limit ($\mu_{ab}\mathcal{E}/\hbar\alpha^{1/2} \ll 1$). Initially, the driving field is far from resonance with the transition, so that $\boldsymbol{\Omega}$ is very near along the w-axis, parallel to $\boldsymbol{\theta}$. Far from resonance, the Rabi frequency is very high, so that $\boldsymbol{\theta}$ precesses rapidly around $\boldsymbol{\Omega}$. As the system is swept through resonance, the vertical component of $\boldsymbol{\Omega}$ crosses through zero. However, the weak-field condition dictates that the sweep through resonance occurs on a time scale that is fast relative to the on-resonance Rabi frequency. Close to resonance, the $\boldsymbol{\theta}$ vector experiences a small torque, approximately (but not exactly) about the u-axis. After the driving vector

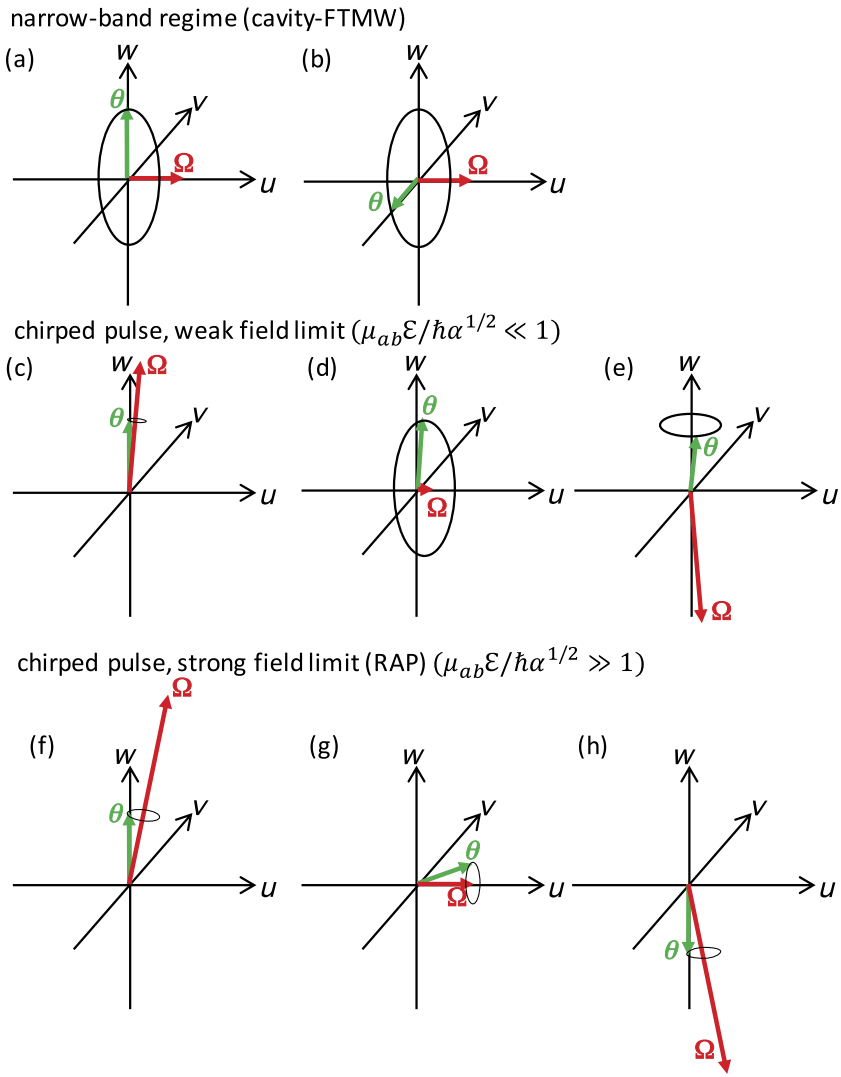

FIG. 2. Schematic representation of the polarization from narrow-band excitation ((a) and (b)), weak-field chirped excitation ((c)-(e)), and strong-field chirped excitation ((f)-(h)) in the Bloch sphere picture. Time increases from left to right. See text for explanation.

has swept past the resonance, it approaches the $-w$ axis, causing $\boldsymbol{\theta}$ to precess about the w-axis, describing a circle with radius proportional to the polarization described by Eq. (3).

The bottom row of Fig. 2 shows the chirped pulse response in the strong driving field limit, known as Rapid Adiabatic Passage (RAP). In this regime, $\mu_{ab}\mathcal{E}/\hbar\alpha^{1/2} \gg 1$, and the Rabi frequency that describes the precession of $\boldsymbol{\theta}$ about $\boldsymbol{\Omega}$ remains fast compared to the rate $\sqrt{\pi\alpha}$ at which $\boldsymbol{\Omega}$ sweeps through resonance. As a result, $\boldsymbol{\theta}$ precesses tightly about $\boldsymbol{\Omega}$ throughout the sweep, and the final result is a population inversion of the system. In contrast to the narrow-band excitation case (top panel of Fig. 2), the $\boldsymbol{\theta}$ vector is rotated about the v-axis, so that the polarization that is induced during the sweep is in-phase (rather than in-quadrature) with the driving field.

Figure 2 underscores some of the special features of the polarization response to a chirped excitation pulse. First, in the strong driving field limit, chirped pulse excitation leads to population inversion via the rapid adiabatic passage mechanism and not to Rabi-cycling, as in the more familiar narrow-band case. Second, there is a difference in phase behavior between the narrow-band and chirped pulse case. In the narrow-band experiment, the polarization is always in-quadrature with the driving field, and therefore the emitted FID is in phase with the driving field, resulting in pure absorptive (or emissive) behavior. However, in the chirped pulse case, $\boldsymbol{\theta}$ may have polarization amplitude along the u-axis, leading to a quadrature component in the emitted FID. This effect increases as the driving field strength is increased, because the behavior of the system transitions from the weak-field to the strong-field case, where $\boldsymbol{\theta}$ follows the u-component of $\boldsymbol{\Omega}$. A Fourier analysis of this effect, which arises because of the importance of non-resonant absorption, is given in Appendix B of Ref. 10.

As pointed out by Schmitz *et al.*,[36] with the help of powerful traveling wave tube (TWT) amplifiers, it has become easy to observe strong field effects in CP-FTMW spectrometers that operate below 40 GHz. These authors demonstrate weak-field relative intensities (Eq. (3)) when using a 75 W excitation pulse, but note strong-field effects when using a 300 W pulse with a $\mu = 4.5$ D molecule in a 2–8 GHz CP-FTMW spectrometer. This suggests that many of the experiments currently being carried out are in a case intermediate between the strong- and weak-field limits. As chirped pulse spectroscopy continues to move into the fields of dynamics and coherent multiple resonance, it will

become increasingly important for researchers to understand the relative intensities and phase behavior.

IV. PERFORMANCE

A. Sensitivity

The most important drawback of CP-FTWM spectroscopy is that, to date, cavity-based techniques provide significantly greater absolute sensitivity. Therefore cavity-FTMW remains as an important complementary technique. Many laboratories now employ both techniques—CP-FTMW is used to obtain a rapid broadband survey spectrum and cavity-FTMW is used to "zoom in" with high sensitivity and high resolution on features of interest.

An explanation sometimes given for the greater sensitivity of Fabry-Pérot cavity based techniques is that the cavity provides passive amplification, not only of the excitation pulse but also of the emitted FID signal. That is, although the TWT amplifiers employed in CP-FTMW spectroscopy are fully capable of providing enough power to optimally polarize coherences within the chirp bandwidth, the technique suffers in sensitivity because it lacks passive amplification of the emitted FID that is provided by cavity-based techniques. An equivalent argument is that the cavity provides a longer effective path length. However, this analysis does not tell the whole story. The primary source of noise in Balle-Flygare type spectrometers is thermal noise from the cavity mirrors and from the surroundings.[37] This blackbody noise limits the noise temperature that can be achieved in the cavity. In other words, the cavity passively amplifies *both* the FID signal *and* the thermal blackbody noise, so that the advantage in signal-to-noise ratio of passive amplification by the cavity is far less than the $Q^{1/2}$ factor of E-field enhancement. In principle, amplification of a broadband FID at the same noise temperature as the cavity should be able to achieve comparable signal-to-noise, although this is difficult to achieve in practice.

However, one must consider that the cavity-based technique is a more mature technology. Over the past 35 years, the design has been refined to optimize performance for detection of trace species. Modern implementations of the Balle-Flygare spectrometer[37,38] employ liquid nitrogen cooling of the cavity mirrors and of the microwave amplifiers to reduce thermal noise. Chirped pulse spectrometers have not yet undergone the same level of optimization and rely on less mature broadband microwave technologies. Rapid advances being made to these technologies and refinements being made to spectrometer designs[39,40] will undoubtedly continue to improve the competitiveness of CP-FTMW techniques.

B. Resolution

Many CP-FTMW spectrometers reported in the literature exhibit poorer frequency resolution than the Balle-Flygare spectrometer. For example, in a recent paper,[41] Peña *et al.* write, "[T]he combination of laser ablation with [CP-FTMW] provides an efficient tool in the analysis of the rotational spectra of biomolecules with high melting points. This technique is complementary to [cavity-based laser ablation molecular beam]-FTMW spectroscopy with superior resolution to resolve the hyperfine structure." However, the reader should not be misled by such statements into thinking that chirped pulse and cavity-based techniques have inherently different limits on resolution. There are three reasons why CP-FTMW spectra are often acquired with lower resolution than cavity-FTMW spectra: experimental geometry, digitizer speed, and signal processing.

The Doppler width due to the velocity spread in a molecular jet expansion is extremely narrow (typically 2–10 kHz for a 10 GHz transition) along the jet propagation direction, but is typically ~10 times wider in the direction perpendicular to the beam propagation direction. In the original Pate design, the chirped microwave pulse propagates perpendicular to the molecular jet expansion, and therefore records Doppler-limited linewidths of ~100 kHz (for a 10 GHz transition). However, in modern implementations of the Balle-Flygare design,[38] the molecular jet is sent into the cavity through a small aperture in one of the mirrors, so that the microwaves and the molecular jet are coaxial. This results in Doppler doubling of each line because the FID is excited by both traveling wave components of the standing wave excitation pulse, i.e., both the component along the molecular propagation (blue shifted) and counter to the molecular propagation (red shifted). Both components exhibit narrow Doppler widths, enabling resolution of small splittings due to nuclear quadrupole moments or nuclear spin-spin interactions.

Because cavity based techniques allow homodyning of the narrow-bandwidth FID to very low frequency, the waveform need not be digitally sampled at a fast rate, and an FID may be recorded for a long duration (many times the T_2 decay time) without overburdening the analog-to-digital converter. On the other hand, in CP-FTMW, the entire broadband spectrum is acquired in every shot, and the FID has a broad bandwidth. To sample a 10 GHz bandwidth at the Nyquist frequency (20 gigasamples/s (GS/s)) for 50 μs, one must digitize 10^6 data points in every shot of the spectrometer. Although modern digitizers are capable of meeting this demand,[42] the digitization process can be rate-limiting in many CP-FTMW implementations. In many laboratories where CP-FTMW is being used as a survey technique alongside cavity-FTMW, the broadband FID is truncated so that resolution is sacrificed for data throughput efficiency.

A more fundamental limitation on CP-FTMW resolution has to do with signal processing. In cavity-based techniques, the narrow-band excitation pulse polarizes all transitions with approximately the same phase. As in FT-NMR, a linear phase correction can be employed to correct the frequency dependent phase accumulation during the delay between the excitation pulse and the FID collection. This ensures that all transitions exhibit an absorptive lineshape in the real part of the Fourier transform. In CP-FTMW, on the other hand, different transitions are excited at different times, so that "phasing" the FID is less straightforward. To complicate the matter further, off-resonant contributions to the phase, the strengths of which are dependent on the individual μ_{ab} transition moments, can make an important contribution if the spectrometer is not operated in the weak-field limit. Although it is, in principle,

possible to apply a digital phase correction,[43] a generic algorithm has not yet been developed, and most practitioners of CP-FTMW instead use a magnitude Fourier transform. Although the use of a window function can significantly improve baseline resolution, the magnitude Fourier transform leads to a lineshape that is inherently slightly broader than the absorptive line because it includes a contribution from the dispersive part.[44]

Despite these considerations, very high resolution can be achieved in coaxial molecular jet implementations of CP-FTMW. For example, in a 8–26 GHz CP-FTMW spectrometer recently described by Jahn *et al.*,[40] the microwave beam is focused along the propagation axis of a molecular jet expansion using a 3-mirror configuration. The microwaves are emitted and received by the same horn antenna. The incoming and outgoing signals are separated using a fast double-throw switch. These authors report linewidths of ~9 kHz for transitions around 9 GHz in 2,6-difluorophenol. (The reported linewidth is limited by closely spaced, unresolvable fine structure due to the nuclear spin-spin interactions among the four hydrogen and two fluorine nuclei.)

C. Relative intensities

A major drawback for cavity-FTMW spectroscopy is the unreliability of relative spectral intensities. The reason is two-fold. First, the broadband spectrum must be scanned in narrowband steps, over the course of several hours or longer. For this reason, the measured relative intensities are sensitive to long-term fluctuations that occur in laboratory conditions. Second, there are uncertainties introduced by the mechanical tuning of the Fabry-Pérot cavity. This second factor can cause step-to-step variation in the cavity Q-factor, so that even lines that are close together in frequency may exhibit significant error in relative intensity.

In CP-FTMW spectroscopy, on the other hand, every frequency element of the spectrum is collected in every shot of the spectrometer. As a result, both long-term and short-term fluctuations in laboratory conditions are averaged out in the relative intensities. Furthermore, the technique does not rely on any mechanically tuned parts, removing this second major source of uncertainty in relative intensities entirely. Although the relative intensity accuracy that was initially reported for CP-FTMW spectroscopy (15%–30%)[1,45,46] may seem modest, this is a significant advantage over cavity-FTMW techniques, which may exhibit order-of-magnitude relative intensity errors. In fact, CP-FTMW spectroscopy has initiated a new trend—authors using chirped pulse methods now routinely provide their audience with figures of their broadband spectra side-by-side with comparisons to calculated relative intensities, a practice that is conspicuously absent in cavity-FTMW work. Most of the error that remains in CP-FTMW intensities is likely caused by accidental standing waves that affect the transmission of the chirped excitation pulse, or by frequency-dependent nonlinearities in the response of the microwave components. As future spectrometers are designed for dynamics applications, where accurate relative-intensity information is crucial, this performance can be significantly improved upon.

V. HIGHLIGHTED ACHIEVEMENTS (TO DATE)

A. Rapid structure determinations on increasingly complex systems

Because of the dramatic increase in the rate of spectral acquisition, CP-FTMW spectroscopy has enabled an increasing number of microwave studies and has pushed the field towards structure determination of increasingly large and complex systems. The body of literature reporting structure determination by CP-FTMW spectroscopy has already grown far too large to provide a complete list of citations here. However, we can briefly discuss statistical trends in microwave spectroscopy over the last decade. Figure 3(a) displays the median number of nuclei contained in species (molecules, complexes, ions, or radicals) whose structure was presented in the microwaves session of the International Symposium on Molecular Spectroscopy, as a function of time. For comparison, Fig. 3(b) displays the number of citations per year received by Ref. 1 in which the original CP-FTMW instrument is described. A clear trend toward structure determination of larger systems is correlated with citations in the literature to chirped-pulse spectroscopy. An increase in median number of nuclei from ~8.5 in the early 2000s to ~13 in the mid-2010s might appear modest. However, the amount of spectroscopic work required in structure determination studies grows extremely rapidly with number of atoms because of the rapid increase in the number of isotopologues and conformers that are involved. There is also a continuing trend toward the microwave spectroscopy of increasingly exotic species such as many-membered clusters[47,48] and reactive intermediates.[49]

B. Implementation of CP-FTMW spectroscopy at higher frequencies

With slight modifications to the original design, CP-FTMW spectroscopy may be readily implemented in lower[50]

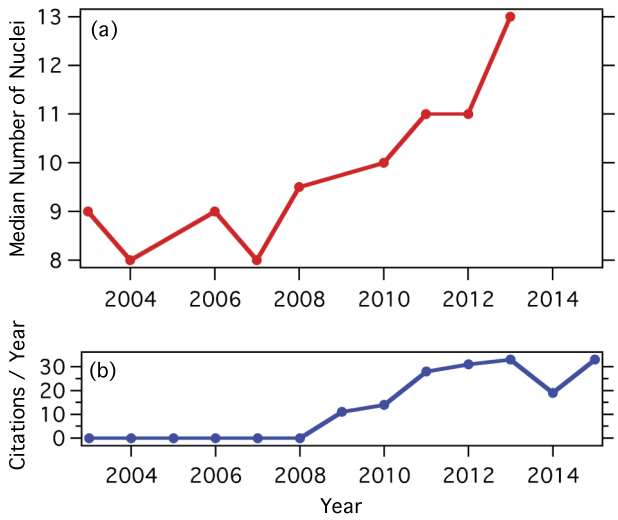

FIG. 3. Panel (a) shows the median number of nuclei contained in chemical species whose structure was presented in the microwaves session of the annual International Symposium on Molecular Spectroscopy over the past decade. For comparison, panel (b) shows the number of citations per year to Ref. 1, where the CP-FTMW spectrometer is described.

and higher[45] microwave bands. However, above ~40 GHz, high-power, full-band TWT amplifiers are not yet available, and optimal polarization of the sample across a broadband frequency range becomes a challenge. Furthermore, since the Doppler effect increases linearly with frequency, the T_2 coherence times become much shorter in the millimeter and sub-millimeter regions, limiting the duration of the excitation pulse that can be used. Most previous millimeter-wave spectrometers involved absorption-based methods.

Chirped-pulse millimeter wave spectrometers operating at 70–102,[51] 260–295,[44] and 546–555.6 GHz[52] have been reported, which make use of active frequency multiplication[44,51] or up-conversion[52] of the arbitrary waveform generator (AWG) output to obtain chirped millimeter-wave pulses. Frequency multiplication has the advantage that both the carrier frequency and the bandwidth of the chirped pulse are multiplied. Broadband heterodyne detection of the signal at microwave frequencies is performed on a fast oscilloscope after down-conversion of the millimeter-wave FID. These spectrometers operate in a regime where signal strength is limited by the relatively low power available for excitation.

In the sub-millimeter wave region, broadband active multiplier chains are typically capable of covering bandwidths of 10%–20% of the center frequency (i.e., bandwidths of 50–100 GHz in the 500 GHz region). The collection of such a broad bandwidth FID signal places severe demands on the oscilloscope hardware bandwidth, pushing the limits of currently available technology and driving up the spectrometer cost. Furthermore, digitization of a ~1 μs FID at a rate of ~100 GS/s becomes impractical, due to the massive data throughput requirements, which limit the data acquisition rate.

These challenges for high-frequency CP-FTMW spectroscopy have been addressed with the introduction of a segmented chirped pulse method.[53] In this method, a two-channel AWG is used. One channel generates a sequence of chirped excitation pulses, which (after passing through a ×72 multiplier chain) sequentially cover the full spectrometer bandwidth (792–859 GHz) in individual segments of 288 MHz bandwidth. The other AWG channel provides the LO used for down-conversion in the detection arm. The LO frequency is stepped so that the heterodyned FID signal is always in the same 288 MHz bandwidth from 4032–4320 MHz and can be digitized quickly on a relatively narrow-band oscilloscope.

C. Chemical reaction dynamics

The idea of using microwave studies for chemical dynamics is not new. More than 80 years ago, microwave spectroscopy was used to determine the precise rate of the ammonia umbrella inversion.[54,55] Numerous modern examples further demonstrate the ability of microwave spectroscopy to characterize the dynamics of systems undergoing large-amplitude chemically relevant motions.[40,47,56] However, CP-FTMW spectroscopy was invented with the specific goal of enabling the characterization of dynamics in laser excited states of complex molecules. In one of their early papers on the technique,[7] the Pate group demonstrated the utility of CP-FTMW for obtaining microwave spectra of laser-excited states of cyclopropane carboxaldehyde, near the threshold to syn ↔ anti isomerization. The two conformers have distinct B rotational constants, but the above-barrier laser-excited states may exhibit rotational character of *both* conformers, the effective rotational constants of which coalesce as the rate of isomerization increases. This observation, designated "dynamic rotation spectroscopy," is analogous to coalescence effects in dynamic NMR spectroscopy of systems undergoing chemical exchange. To measure the effect in cyclopropane carboxaldehyde, it was necessary to obtain a microwave spectrum covering the interval of several GHz that separates the characteristic $J = 2 \leftarrow 1$ rotational transition frequency of the two isomers, as a function of vibrational excitation energy. The authors emphasize that with the capabilities of CP-FTMW, each broadband rotational spectrum can be quickly acquired (in a matter of seconds) so that the high-resolution IR laser scan over the region of interest could be completed in 52 h. On the other hand, each broadband scan of a cavity-FTMW spectrometer requires hours of operation, and acquisition of the same dataset with a cavity spectrometer would have required 27 yr.

Because of its ability to measure accurate relative intensity information of many species simultaneously, CP-FTMW spectroscopy is well suited to the measurement of product distributions from reactions induced by photolysis or flash pyrolysis, an area of experimental reaction dynamics that has more traditionally belonged to the domain of techniques such as photoionization mass spectrometry (PIMS). However, unlike mass spectrometry-based techniques, microwave spectroscopy can provide conformer-specific identification of the nascent reaction products and does not rely on *a priori* knowledge of the product-specific photoionization cross sections. Once the rotational constants are known, it is usually unambiguous to assign microwave transitions to individual species, even in a complex mixture of reaction products. Prozument *et al.*[5,46] have demonstrated the capability of chirped-pulse millimeter wave spectroscopy to determine product branching ratios and nascent vibrational distributions from the flash pyrolysis of ethyl nitrite, and Kidwell *et al.*[49] have demonstrated the effectiveness of CP-FTMW to identify and determine the structure of the reactive intermediate cyclopentadienone in the flash pyrolysis of *o*-phenylene sulfite.

Recent work by the Arthur Suits group has taken the application of microwave spectroscopy to the study of chemical reaction kinetics a step further.[6,57,58] Bimolecular reactions, initiated by a pulsed photolysis laser, are carried out at ~7 mbar pressure and low temperature (~20 K) in a pulsed uniform supersonic flow. The appearance of reaction products is probed as a function of time by applying a series of chirped pulse excitations, enabling the measurement of cold bimolecular reaction kinetics on a μs timescale.

D. Coherently detected, frequency-agile multiple resonance

Another huge advantage offered by CP-FTMW spectroscopy is the ability to streamline the acquisition of double-resonance information and to perform frequency-agile

coherent double resonance experiments that make use of phase as well as intensity information. As microwave spectroscopy moves in the direction of larger and more complicated systems, the spectra also become more challenging to interpret. Double resonance can be used as a tool to provide both unequivocal assignment and increased spectral resolution. Double resonance and fully coherent 2D spectroscopies are routinely employed in NMR as invaluable tools for the interpretation of complex spectra. However, microwave double-resonance techniques are far less commonplace, because the process of checking for double resonance signals one-microwave-frequency-at-a-time is inefficient and tedious.

1. Multiplexed microwave-optical double resonance

The Pate group first demonstrated the use of CP-FTMW spectroscopy to multiplex the acquisition of double resonance data in their MW-IR work on cyclopropane carboxaldehyde, discussed above.[7] Our group at MIT has extended this work, using the frequency-agile pulse generation capabilities of our chirped pulse spectrometer to implement multiplexed millimeter-wave/optical double resonance using coherent FID detection.[8] The technique uses a series of single-frequency pulses to simultaneously detect laser-induced depletion in population (or coherence) of many rotational levels of the lower-state. The result is a laser absorption spectrum, acquired in a single scan of the laser, that comes with all rotational assignments attached. We have used the technique to assign perturbed bands of the $\tilde{C}$ state of SO_2 that were challenging to interpret solely from laser-induced fluorescence data. We have also explored the possibility of multiplexing the coherence-converted population transfer (CCPT) technique,[39,59] which uses a phase-sensitive pulse sequence to obtain a background-free FID-detected double resonance signal.

2. Coherent manipulation of Rydberg states

Our group has also used multiple resonance for the coherent detection and manipulation of pure electronic transitions in highly excited Rydberg states of atoms[60,61] and molecules.[10] At high principal quantum number ($n \approx 30$–40), Rydberg series become closely spaced and $\Delta n = 1$ electronic transitions fall in the millimeter-wave and microwave spectral regions. Because these transitions possess ~1000 D electric dipole transition moments, coherent microwave experiments on Rydberg states fall into a qualitatively different regime than rotational microwave spectroscopy, which typically involves ~1 D transition moments. Rydberg-Rydberg transitions can be strongly polarized by even a weak excitation pulse, and typically the emitted FID is comparable in strength to the excitation pulse. As a result, Rydberg molecules can communicate with one another coherently via a common oscillatory electric field, leading to the possibility of studying cooperative absorption and emission of radiation in Rydberg gases with number densities $\gtrsim 10^5$ cm^{-3}.[62] In recent work, Rydberg number densities of $\gtrsim 10^7$ cm^{-3} have revealed strong cooperative emission in systems initially prepared in an unstable equilibrium. The emission is stabilized by crafting very weak "tipping" millimeter-wave pulses to initiate the emission. The time-dependent intensity and frequency behavior of single-shot FIDs reveals the nature of cooperative dynamics at varying number densities, generated by shot-to-shot fluctuations in the laser pulse intensity and molecular beam conditions.[63]

The study of molecular Rydberg states is also fundamental to the understanding of chemistry because the physical mechanisms of electron collisions with ion cores governs (from a reductionist perspective) virtually all of chemistry. One of the challenges of performing coherent microwave experiments on molecular Rydberg states is that the low-l (core penetrating) Rydberg states readily accessible by laser excitation schemes typically have extremely short lifetimes due to predissociation. Our group has made progress toward overcoming this hurdle using sequences of millimeter-wave pulses to rapidly transfer population to successively higher-l (core nonpenetrating) states via ladder schemes, and we have demonstrated Stark techniques for characterizing the degree of core penetration in Rydberg states of molecules.[10,61] Zhou and co-workers[10] have also developed methodology for using sequences of chirped millimeter wave pulses to "map" entire manifolds of Rydberg levels via multiple resonance pyramid schemes, which start with a single laser excited level and then sequentially apply pulses that excite all states connected via strong transition moments to the previously populated Rydberg levels. The direction of a transition (up vs. down) in such an experiment can be extracted from the phase of the emitted FID.

3. Radiofrequency-microwave and microwave-microwave multiple resonance

Schmitz *et al.*[64] demonstrated the use of CP-FTMW spectroscopy for RF-MW double resonance between low-frequency (~300 MHz) and higher-frequency (~4 GHz) rotational transitions. One advantage of using chirped pulse spectroscopy is that it can be used to multiplex the acquisition of such double resonance data over the entire microwave spectrum. However, Schmitz *et al.* show that coherent microwave detection provides a further advantage. As a result of AC-Stark effects (Autler-Townes splittings) induced by the RF pulse, the frequency of the microwave FID is blue-shifted or red-shifted, and the direction of the shift changes sign as the RF pulse is tuned across resonance. The frequency shift leads to a phase shift in the coherently detected FID. The double resonance signal can be much more sensitively and precisely detected by monitoring the phase shift than by the more conventional approach of monitoring changes induced in the microwave intensities.

A final area of multiple resonance introduced recently involves the use of microwave three-wave mixing as a detector of chirality in molecules with C_1 symmetry.[9,65–67] Although enantiomers have the same rotational constants and thus the same transition frequencies, they differ in the sign of the scalar triple product $\mu_a \cdot \mu_b \times \mu_c$. (Nonzero permanent a-, b-, and c-dipole moments can only occur simultaneously in chiral molecules with C_1 symmetry.) Microwave three-wave mixing

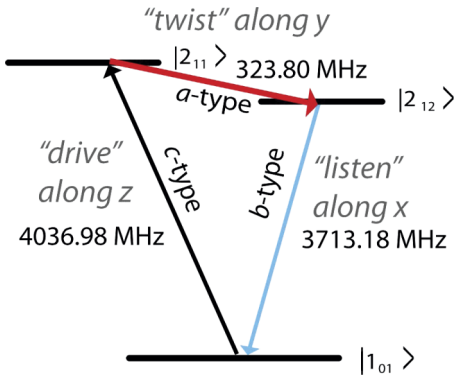

FIG. 4. A three-wave mixing cycle for the detection of enantiomeric excess in menthone, reprinted with permission from V. A. Shubert, D. Schmitz, and M. Schnell, "Enantiomer-sensitive spectroscopy and mixture analysis of chiral molecules containing two stereogenic centers—Microwave three-wave mixing of menthone," J. Mol. Spectrosc. **300**, 31–36 (2014). Copyright 2014 Elsevier.

makes use of a "cycle" of three rotational levels, which are connected via a sequence of *a*-, *b*-, and *c*-type transitions, as shown in Figure 4. Solution of the Maxwell-Bloch equations for a three level system shows that subsequent polarization of the ρ_{ab} coherence in the Z laboratory frame direction and ρ_{bc} in the Y laboratory frame direction leads to ρ_{ac} coherence in the X laboratory frame direction, the phase of which depends on the phase of the first two excitation pulses and on the sign of $\mu_a \cdot \mu_b \times \mu_c$. The X-polarized FID signal from the pair of enantiomers will be 180° out of phase. Thus, the signal is proportional to enantiomeric excess and perfectly cancels for a racemic mixture. Unlike most optical methods for detection of chirality, three-wave mixing is fully electric dipole allowed and therefore yields strong signals, approaching optimal $\sim\pi/2$ polarization.[68] It has the further advantage that diastereomers in complex mixtures can be easily resolved because they have different rotational constants.[67] However, because three microwave/RF frequencies are used simultaneously, the technique is incompatible with narrow-band cavity-based spectrometers.

VI. OUTLOOK

Since its invention in the Pate lab ten years ago, many laboratories have built new spectrometers, or modified existing instruments, to adopt the CP-FTMW technique. The technique provides a huge advantage because it increases the rate at which a broadband microwave spectrum can be obtained by several orders of magnitude. However, because the more mature technologies employed in modern implementations of Balle-Flygare type spectroscopy typically outperform CP-FTMW in absolute sensitivity and frequency resolution, cavity-FTMW remains an important complementary technique. Nevertheless, we believe the limitations to the sensitivity and resolution of CP-FTMW spectroscopy are practical rather than fundamental in nature. Therefore, as researchers gain experience with the technique and build future generations of spectrometers with constantly improving broadband microwave technologies, CP-FTMW spectroscopy is likely to become increasingly competitive. Furthermore, whereas the fast AWG, high power TWT amplifier, and broadband oscilloscope used in the original implementation are bulky and expensive, new, chip-based designs that use digital synthesizers, solid state amplifiers, and fast digitizers can reduce the instrument cost by ~2 orders of magnitude.[42]

However, the true strength of the CP-FTMW innovation does not lie in the mere ability to collect microwave spectra at unprecedented rates. By freeing microwave spectroscopy from the narrowband cavity and standardizing the use of frequency-agile pulse generation and broadband FID detection, CP-FTMW spectroscopy opens new horizons for the field. Already, the chirped pulse innovation has led to novel classes of microwave experiments, ranging from 3-wave mixing schemes for chirality detection to broadband chemical sensing for monitoring reaction kinetics in the time domain. The next generation of microwave spectroscopists will enter a field in which the creative design of coherent experiments to probe molecular dynamics is less constrained than ever. Fully coherent 2D CP-FTMW spectroscopy has already been explored,[69] but currently remains an undeveloped area of research. The development of such techniques will provide the means not only to diagnose and disentangle complex spectra, but might also enable unique new experiments, such as time-resolved tracking of the moments of inertia of coherent states.

ACKNOWLEDGMENTS

R.W.F. acknowledges support from U.S. Department of Energy, Office of Science, Chemical Sciences Geosciences and Biosciences Division of the Basic Energy Sciences Office (Grant No. DE-FG0287ER13671), the National Science Foundation (Grant No. CHE-1361865), and from the American Chemical Society Petroleum Research Fund (Grant No. 50650-ND6). G.B.P. acknowledges support from a National Science Foundation Graduate Research Fellowship.

[1]G. G. Brown, B. C. Dian, K. O. Douglass, S. M. Geyer, S. T. Shipman, and B. H. Pate, Rev. Sci. Instrum. **79**, 053103 (2008).
[2]G. G. Brown, B. C. Dian, K. O. Douglass, S. M. Geyer, and B. H. Pate, J. Mol. Spectrosc. **238**, 200 (2006).
[3]C. Cabezas, M. A. T. Robben, A. M. Rijs, I. Peña, and J. L. Alonso, Phys. Chem. Chem. Phys. **17**, 20274 (2015).
[4]C. Pérez, D. P. Zaleski, N. A. Seifert, B. Temelso, G. C. Shields, Z. Kisiel, and B. H. Pate, Angew. Chem., Int. Ed. **53**, 14368 (2014).
[5]K. Prozument, Y. V. Suleimanov, B. Buesser, J. M. Oldham, W. H. Green, A. G. Suits, and R. W. Field, J. Phys. Chem. Lett. **5**, 3641 (2014).
[6]C. Abeysekera, B. Joalland, N. Ariyasingha, L. N. Zack, I. R. Sims, R. W. Field, and A. G. Suits, J. Phys. Chem. Lett. **6**, 1599 (2015).
[7]B. C. Dian, G. G. Brown, K. O. Douglass, and B. H. Pate, Science **320**, 924 (2008).
[8]G. B. Park, C. C. Womack, A. R. Whitehill, J. Jiang, S. Ono, and R. W. Field, J. Chem. Phys. **142**, 144201 (2015).
[9]D. Patterson and J. M. Doyle, Phys. Rev. Lett. **111**, 023008 (2013).
[10]Y. Zhou, D. D. Grimes, T. J. Barnum, D. Patterson, S. L. Coy, E. Klein, J. S. Muenter, and R. W. Field, Chem. Phys. Lett. **640**, 124 (2015).
[11]R. H. Dicke and R. H. Romer, Rev. Sci. Instrum. **26**, 915 (1955).
[12]R. M. Somers, T. O. Poehler, and P. E. Wagner, Rev. Sci. Instrum. **46**, 719 (1975).
[13]J. Ekkers and W. H. Flygare, Rev. Sci. Instrum. **47**, 448 (1976).
[14]M. L. Unland and W. H. Flygare, J. Chem. Phys. **45**, 2421 (1966).
[15]T. Amano and T. Shimizu, J. Phys. Soc. Jpn. **35**, 237 (1973).
[16]B. Macke and P. Glorieux, Chem. Phys. Lett. **18**, 91 (1973).

[17]K. Tanaka and E. Hirota, J. Mol. Spectrosc. **59**, 286 (1976).
[18]S. L. Coy, J. Chem. Phys. **63**, 5145 (1975).
[19]J. C. McGurk, R. T. Hofmann, and W. H. Flygare, J. Chem. Phys. **60**, 2922 (1974).
[20]T. L. Weatherly, Q. Williams, and F. Tsai, J. Chem. Phys. **61**, 2925 (1974).
[21]J. H.-S. Wang, J. M. Levy, S. G. Kukolich, and J. I. Steinfeld, Chem. Phys. **1**, 141 (1973).
[22]J. C. McGurk, T. G. Schmalz, and W. H. Flygare, J. Chem. Phys. **60**, 4181 (1974).
[23]T. J. Balle, E. J. Campbell, M. R. Keenan, and W. H. Flygare, J. Chem. Phys. **71**, 2723 (1979).
[24]T. J. Balle and W. H. Flygare, Rev. Sci. Instrum. **52**, 33 (1981).
[25]A. C. Legon and D. J. Millen, Faraday Discuss. Chem. Soc. **73**, 71 (1982).
[26]A. C. Legon, Annu. Rev. Phys. Chem. **34**, 275 (1983).
[27]A. C. Legon, J. Mol. Struct. **266**, 21 (1992).
[28]A. Bauder, J. Mol. Struct. **408/409**, 33 (1997).
[29]Y. Ohshima and Y. Endo, Chem. Phys. Lett. **256**, 635 (1996).
[30]M. C. McCarthy and P. Thaddeus, Chem. Soc. Rev. **30**, 177 (2001).
[31]Y. Kawashima, T. Usami, N. Ohashi, R. D. Suenram, J. T. Hougen, and E. Hirota, Acc. Chem. Res. **39**, 216 (2006).
[32]J. Alonso and J. C. López, "Microwave spectroscopy of biomolecular building blocks," in *Gas-Phase IR Spectroscopy and Structure of Biological Molecules*, edited by A. M. Rijs and J. Oomens (Springer, 2015).
[33]J. C. McGurk, T. G. Schmalz, and W. H. Flygare, in *Advances in Chemical Physics*, edited by S. A. Rice and I. Prigogine (Academic, New York, 1974), Chap. 1.
[34]G. B. Park and R. W. Field, J. Mol. Spectrosc. **312**, 54 (2015).
[35]L. Allen and J. H. Eberly, *Optical Resonance and Two-Level Atoms* (Dover, New York, 1987).
[36]D. Schmitz, V. A. Shubert, T. Betz, and M. Schnell, J. Mol. Spectrosc. **280**, 77 (2012).
[37]J.-U. Grabow, E. S. Palmer, M. C. McCarthy, and P. Thaddeus, Rev. Sci. Instrum. **76**, 093106 (2005).
[38]J.-U. Grabow, W. Stahl, and H. Dreizler, Rev. Sci. Instrum. **67**, 4072 (1996).
[39]J. L. Neill, K. O. Douglass, B. H. Pate, and D. W. Pratt, Phys. Chem. Chem. Phys. **13**, 7253 (2011).
[40]M. K. Jahn, D. A. Dewald, D. Wachsmuth, J.-U. Grabow, and S. C. Mehrotra, J. Mol. Spectrosc. **280**, 54 (2012).
[41]I. Peña, M. Varela, V. G. Franco, J. C. López, C. Cabezas, and J. L. Alonso, J. Phys. Chem. A **118**, 11373 (2014).
[42]I. A. Finneran, D. B. Holland, P. B. Carroll, and G. A. Blake, Rev. Sci. Instrum. **84**, 083104 (2013).
[43]F. Xian, C. L. Hendrickson, G. T. Blakney, S. C. Beu, and A. G. Marshall, Anal. Chem. **82**, 8807 (2010).
[44]A. L. Steber, B. J. Harris, J. L. Neill, and B. H. Pate, J. Mol. Spectrosc. **280**, 3 (2012).
[45]D. P. Zaleski, J. L. Neill, M. T. Muckle, N. A. Seifert, P. B. Carroll, S. L. W. Weaver, and B. H. Pate, J. Mol. Spectrosc. **280**, 68 (2012).
[46]K. Prozument, G. B. Park, R. G. Shaver, A. K. Vasiliou, J. M. Oldham, D. E. David, J. S. Muenter, J. F. Stanton, A. G. Suits, G. B. Ellison, and R. W. Field, Phys. Chem. Chem. Phys. **16**, 15739 (2014).
[47]C. Pérez, M. T. Muckle, D. P. Zaleski, N. A. Seifert, B. Temelso, G. C. Shields, Z. Kisiel, and B. H. Pate, Science **336**, 897 (2012).
[48]G. Feng, L. Evangelisti, I. Cacelli, L. Carbonaro, G. Prampolini, and W. Caminati, Chem. Commun. **50**, 171 (2014).
[49]N. M. Kidwell, V. Vaquero-Vara, T. K. Ormond, G. T. Buckingham, D. Zhang, D. N. Mehta-Hurt, L. McCaslin, M. R. Nimlos, J. W. Daily, B. C. Dian, J. F. Stanton, G. B. Ellison, and T. S. Zwier, J. Phys. Chem. Lett. **5**, 2201 (2014).
[50]J. L. Neill, S. T. Shipman, L. Alvarez-Valtierra, A. Lesarri, Z. Kisiel, and B. H. Pate, J. Mol. Spectrosc. **269**, 21 (2011).
[51]G. B. Park, A. H. Steeves, K. Kuyanov-Prozument, J. L. Neill, and R. W. Field, J. Chem. Phys. **135**, 024202 (2011).
[52]E. Gerecht, K. O. Douglass, and D. F. Plusquellic, Opt. Express **19**, 8973 (2011).
[53]J. L. Neill, B. J. Harris, A. L. Steber, K. O. Douglass, D. F. Plusquellic, and B. H. Pate, Opt. Express **21**, 19743 (2013).
[54]C. E. Cleeton and N. H. Williams, Phys. Rev. **45**, 234 (1934).
[55]B. Bleaney and R. P. Penrose, Nature **157**, 339 (1946).
[56]A. J. Thomas, M. M. Serafin, A. A. Ernst, R. A. Peebles, and S. A. Peebles, J. Mol. Spectrosc. **289**, 65 (2013).
[57]J. M. Oldham, C. Abeysekera, B. Joalland, L. N. Zack, K. Prozument, I. R. Sims, G. B. Park, R. W. Field, and A. G. Suits, J. Chem. Phys. **141**, 154202 (2014).
[58]C. Abeysekera, L. N. Zack, G. B. Park, B. Joalland, J. M. Oldham, K. Prozument, N. M. Ariyasingha, I. R. Sims, R. W. Field, and A. G. Suits, J. Chem. Phys. **141**, 214203 (2014).
[59]S. Twagirayezu, T. N. Clasp, D. S. Perry, J. L. Neill, M. T. Muckle, and B. H. Pate, J. Phys. Chem. A **114**, 6818 (2010).
[60]K. Prozument, A. P. Colombo, Y. Zhou, G. B. Park, V. S. Petrović, S. L. Coy, and R. W. Field, Phys. Rev. Lett. **107**, 143001 (2011).
[61]A. P. Colombo, Y. Zhou, K. Prozument, S. L. Coy, and R. W. Field, J. Chem. Phys. **138**, 014301 (2013).
[62]Y. Zhou, Mol. Phys. **110**, 1909 (2012).
[63]D. D. Grimes, S. L. Coy, T. J. Barnum, Y. Zhou, S. F. Yelin, and R. W. Field, "Direct single-shot observation of millimeter wave superradiance in Rydberg-Rydberg transitions" (unpublished).
[64]D. Schmitz, V. A. Shubert, D. Patterson, A. Krin, and M. Schnell, J. Chem. Phys. Lett. **6**, 1493 (2015).
[65]D. Patterson, M. Schnell, and J. M. Doyle, Nature **497**, 475 (2013).
[66]S. Lobsiger, C. Perez, L. Evangelisti, K. K. Lehmann, and B. H. Pate, J. Phys. Chem. Lett. **6**, 196 (2015).
[67]V. A. Shubert, D. Schmitz, and M. Schnell, J. Mol. Spectrosc. **300**, 31 (2014).
[68]J.-U. Grabow, Angew. Chem., Int. Ed. **52**, 11698 (2013).
[69]D. S. Wilcox, K. M. Hotopp, and B. C. Dian, J. Phys. Chem. A **115**, 8895 (2011).